

# Sequential Attack Impairs Security in Device-independent Quantum Key Distribution

Pritam Roy,<sup>1,\*</sup> Souradeep Sasmal,<sup>2,†</sup> Subhankar Bera,<sup>1,‡</sup>  
Shashank Gupta,<sup>3,4,§</sup> Arup Roy,<sup>5,¶</sup> and A. S. Majumdar<sup>1,\*\*</sup>

<sup>1</sup>*S. N. Bose National Centre for Basic Sciences,  
Block JD, Sector III, Salt Lake, Kolkata 700 106, India*

<sup>2</sup>*Institute of Fundamental and Frontier Sciences,  
University of Electronic Science and Technology of China, Chengdu 611731, China*

<sup>3</sup>*Okinawa Institute of Science and Technology Graduate University, Okinawa, Japan*

<sup>4</sup>*QuNu Labs Pvt. Ltd., M. G. Road, Bengaluru, Karnataka 560025, India*

<sup>5</sup>*Department of Physics, A B N Seal College Cooch Behar, West Bengal 736101, India*

Device-independent quantum key distribution (DI-QKD) leverages nonlocal correlations to securely establish cryptographic keys between two honest parties while making minimal assumptions about the underlying systems. The security of DI-QKD relies on the validation of quantum theory, with Bell violations ensuring the inherent unpredictability of the observed statistics, independent of the trustworthiness of the devices. While traditional QKD attacks are generally categorised as individual, collective, or coherent attacks, we introduce a novel attack strategy—the sequential attack. In this approach, Eve intercepts the transmitted quantum particle, performs an unsharp measurement to preserve the Bell violation between the honest parties, and disguises her interference as noise. Such a strategy enables Eve to extract substantial information about the key, even without performing collective measurements. Furthermore, when combined with collective attack, this strategy significantly reduces the secure key rate and, under certain conditions, can render it to zero. We show that within specific ranges of Bell violations and quantum bit error rates, the cumulative effect of sequential and collective attacks poses a stronger threat to DI-QKD security than collective attacks alone. These findings underscore the vulnerability of DI-QKD to real-world imperfections, emphasising that Bell nonlocality alone is insufficient to guarantee security in practical implementations.

## I. INTRODUCTION

The aim of key distribution is to securely share a secret key between two parties, say Alice and Bob, to enable confidential communication. In accordance with Kirkhoff’s Principle—‘the enemy knows the system’—the security of any cryptosystem must rely exclusively on the secrecy of the key, rather than on the algorithm, method, or device employed [1, 2]. Beyond the foundational insights into the interpretation of quantum theory, the violation of Bell inequalities offers the requisite device independence for key distribution protocols, ensuring security even when the devices utilised are untrusted [3–6].

Bell’s work [7, 8] elucidates that when quantum statistics violate a Bell inequality, it implies that such statistics cannot be generated by any pre-shared strategy—more precisely, through Local Operations and Shared Randomness (LOSR) [9, 10]. This renders the statistics inherently unpredictable, irrespective of the adversary’s knowledge of the underlying processes [11]. Since violations of Bell inequalities can be verified solely through observed statistics, this verification serves as a black-box test of unpredictability, thereby pioneering the physics behind Device-

Independent Quantum Key Distribution (DI-QKD) with minimal assumptions [3, 4, 12–21]. The security of DI-QKD is thus predicated solely on the validation of quantum theory, allowing users to forgo trust in the inner workings of the devices and ensuring security against any adversary constrained by quantum theory.

Traditional QKD attacks typically focus on the quantum channel during transmission and can be categorised into individual [22–24], collective [13, 25], and coherent [26] attacks. These attacks presume that adversaries have control over the preparation and measurement devices, potentially tampering with them during manufacture. One might contend that if one party prepares the quantum system and shares a subsystem with the other, Eve, the adversary, would lose control over the preparation device, thereby diminishing her ability to predict the generated key. Additionally, with only one particle traversing the channel instead of two, the noise could be reduced, potentially enhancing the noise tolerance of DI-QKD protocols.

However, by manipulating the quantum channel, Eve could regain control. This raises the question: what strategy would Eve employ? In this work, we analyse a noise-masking attack, wherein Eve disguises her interference as the expected noise. In this scenario, Eve intercepts one of the particles and performs an unsharp measurement, ensuring that the Bell violation between Alice and Bob persists. Even without initial control over the source, Eve can still generate her desired mixed state through this specific sequential attack.

\* roy.pritamphy@gmail.com

† souradeep.007@gmail.com

‡ berasanu007@gmail.com

§ shashankg687@gmail.com

¶ arup145.roy@gmail.com

\*\* archan@bose.res.in

Intuitively, one might expect that Eve’s measurement would disturb the quantum state, preventing Alice and Bob from observing a violation of a Bell inequality, such as the CHSH inequality [27] in the simplest scenario involving two parties, two measurements per party, two outcomes per measurement (2-2-2). On the contrary, recent findings reveal that Bell nonlocality can indeed be shared between Alice and multiple independent Bobs through sequential violations of the CHSH inequality based on unsharp measurements [28–33].

Recently, there has been a notable surge of interest in the sequential sharing of quantum correlations, especially in areas such as entanglement [34–37], steering [38–42], multi-setting Bell-nonlocality [43], Network Nonlocality [44–47], coherence [48], and contextuality [49, 50], with extensions to multipartite scenarios [51–55]. Several experiments have corroborated this phenomenon [34, 56–60], underscoring its significance to both foundational quantum research and practical applications. Applications of sequential quantum correlations encompass randomness generation [61–64], reducing classical communication costs [65], quantum teleportation [66], random access codes [67, 68], self-testing of unsharpness parameters [69–72], and Remote state preparation [73]. The above findings motivate the importance of further analysing the role of unsharp measurements in sequential quantum correlation scenarios.

In this work, we demonstrate how Eve can exploit the phenomenon of sequential sharing of nonlocality to acquire additional information regarding the shared key in DI-QKD. This strategy uncovers the potential for a non-trivial unsharp measurement attack, which has previously been considered relevant only in prepare-and-measure QKD protocols [2, 74–76]. Our analysis involves estimating the key rate with suitable quantifiers [12, 13, 77], sequential CHSH violations, and the quantity of Quantum Bit Error Rate (QBER). We investigate two pertinent scenarios under one-way communication: (1) a sequential unsharp measurement attack where Alice sends the entangled particle to Bob, and Eve intervenes prior to its arrival at Bob’s Lab (Sec. III), and (2) the cumulative effect of the sequential and collective attacks (Sec. IV).

In a standard collective attack, Eve controls the source, distributing a mixed entangled state to Alice and Bob while retaining its purification in a quantum memory for subsequent collective measurement. In a sequential attack, Eve intercepts the photon sent from Alice to Bob in each round, performs a measurement (Sec. III) to maximise information gain while preserving the nonlocality between Alice and Bob, and forwards the post-measurement state to Bob. We extend this approach to analyse the impact of combined sequential and collective attacks on the key rate (Sec. IV). In the latter scenario, Eve performs the sequential measurement, prepares the ancilla states based on the observed outcome statistics, and stores the ancilla for a subsequent collective measurement, thereby integrating the characteristics of both

attack strategies.

To lay the foundations of our findings, we first validate the sequential attack and evaluate the secure key rate under the assumption that Eve employs unsharp measurements with a biased parameter to maximise information gain. Our results indicate that the key rate in the purely sequential attack scenario surpasses that of a collective attack. However, by making slight adjustments to the QBER while maintaining the same CHSH violation, Eve can extract a substantial amount of information regarding the key without performing collective measurements on her subsystem. Furthermore, when the sequential attack is combined with collective attacks, it becomes significantly more potent. In this combined attack, Eve’s knowledge is evolved into a non-linear function of the biased parameter. Our analysis leads to the identification of a region where the key rate remains positive under a collective attack but becomes zero under the combined attack, thereby highlighting a more formidable threat to the security of DI-QKD and providing a tighter estimate of the key rate (Sec. IV).

Even though Bell inequality violations and secure key rates are frequently perceived as concomitant features, our work supports recent findings, consistent with Farkas et al.’s [78] demonstration that nonlocality alone is insufficient for DI-QKD security, as illustrated by a convex combination eavesdropping attack on Werner states. Our results extend this analysis by considering a different type of attack, confirming that nonlocality alone does not guarantee security in DI-QKD. We begin with a brief recap of the collective attack scenario [13, 25] (Sec. II), which will be used as reference for the analysis presented in the subsequent sections.

## II. DI-QKD UNDER COLLECTIVE ATTACKS

Alice prepares a bipartite entangled state,  $\rho \in \mathcal{L}(\mathcal{H}_A \otimes \mathcal{H}_B)$ , and shares one-half with Bob via a quantum channel. This process spans several rounds  $N$ , each assumed independent, resulting in a shared state  $\otimes_N \rho$ . In each round, Alice randomly selects one of  $m_A$  local measurements,  $\{A_x : x \in [m_A]\}$ , recording outcomes  $a \in \{1, 2, \dots, d_A\}$ . Similarly, Bob selects from  $m_B$  local measurements,  $\{B_y : y \in [m_B]\}$ , with outcomes  $b \in \{1, 2, \dots, d_B\}$ . The resulting statistics are captured by a vector in real number space,  $\mathcal{P} \equiv \{p(a, b|x, y)\} \in \mathbb{R}^{m_A m_B d_A d_B}$ , where  $P(a, b|x, y)$  denotes the joint conditional probability of obtaining outcome-pair  $(a, b)$ .

In quantum theory, measurements  $A_x$  and  $B_y$  are described by Positive-Operator-Valued-Measures (POVMs),  $A_x \in \mathcal{L}(\mathcal{H}^A) \equiv \{A_{a|x}\}$  and  $B_y \in \mathcal{L}(\mathcal{H}^B) \equiv \{B_{b|y}\}$ , respectively. The joint conditional probability follows the Born rule:  $p(a, b|x, y, \rho) = \text{Tr}[\rho A_{a|x} \otimes B_{b|y}]$ , where  $A_{a|x}$  and  $B_{b|y}$  are corresponding projectors for outcomes  $a$  and  $b$ . After measurement, Alice and Bob publicly disclose their measurement settings and a subset of outcomes to estimate joint statistics, crucial for detect-

ing violations of the Bell inequality. Such violations of a Bell inequality underpin the establishment of a private key between Alice and Bob [79].

Here, we consider that Alice selects from three measurement settings  $(A_0, A_1, A_2)$  and Bob from two  $(B_1, B_2)$ . Using  $A_1, A_2$  and  $B_1, B_2$  respectively, Alice and Bob test nonlocality in the simplest 2-2-2 Bell scenario by observing violations of the following CHSH inequality [27]

$$S = \langle A_1 B_1 \rangle + \langle A_1 B_2 \rangle + \langle A_2 B_1 \rangle - \langle A_2 B_2 \rangle \leq \frac{2}{L} \quad (1)$$

where  $\langle A_x B_y \rangle = \sum_{a,b} (-1)^{a+b} p(a, b | x, y, \rho)$  with  $a, b \in \{+1, -1\}$ .

Finally, after discarding the dataset used in the spot-checking phase, Alice and Bob extract a raw key from the pair  $(A_0, B_1)$ . In the presence of eavesdropping, the information accessible to Eve is bounded by the parameters  $\mathcal{S}$  and the quantum bit error rate (QBER),  $Q = p(a \neq b | A_0, B_1, \rho)$  [13]. Subsequently, Alice and Bob distill a secure key from the raw data through classical post-processing via a public channel [13].

In the context of collective attacks, where Eve's interventions are characterised by one-way classical post-processing from Bob to Alice, the Devetak-Winter rate [12] is a fundamental metric for the secret key rate, given by

$$r \geq 1 - H(Q) - \chi(B_1 : E) \quad (2)$$

Here,  $H$  is the binary entropy with  $H(x) = -x \log_2 x - (1-x) \log_2 (1-x)$ , and  $H(Q) = 1 - \mathcal{I}(A_0 : B_1)$  where  $\mathcal{I}(A_0 : B_1)$  is the mutual information between Alice and Bob.  $\chi(B_1 : E)$  denotes the Holevo quantity, given by  $\chi(B_1 : E) = S(\rho_E) - \frac{1}{2} \sum_{b_1=\pm 1} S(\rho_{E|b_1})$ , between Eve and Bob, which is upper bounded as  $\chi(B_1 : E) \leq H\left(\frac{1+\sqrt{(S/2)^2-1}}{2}\right)$ , with  $\mathcal{S}$  denoting the CHSH value [13].

Consider a scenario where Alice prepares a maximally entangled two-qubit state,  $\rho = |\Phi^+\rangle\langle\Phi^+|$  and shares one-half of the entangled qubit with Bob through a quantum channel. They intend to implement the following optimal measurement directions to achieve the optimal CHSH value  $2\sqrt{2}$ .

$$A_0 = B_1 = \sigma_z; A_x = \frac{1}{\sqrt{2}}[B_1 + (-1)^x B_2]; B_2 = \sigma_x; \quad (3)$$

where  $x \in \{1, 2\}$ . The measurement pair  $(A_0, B_1)$  is employed by Alice and Bob for the evaluation of the QBER. In the presence of a collective attack by Eve, the prepared state is assumed to take the form of a mixed entangled two-qubit state, given by

$$\tilde{\rho} = \frac{1}{4} \left( 2 + \sqrt{1 - \alpha^2} \right) |\Phi^+\rangle\langle\Phi^+| + \frac{1}{4} |\Phi^-\rangle\langle\Phi^-| + \frac{1}{4} \left( 1 - \sqrt{1 - \alpha^2} \right) |\Psi^+\rangle\langle\Psi^+| \quad \forall \alpha \in [0, 1] \quad (4)$$

Note that in [13], a specific example of a two-qubit Werner state was used to compute the key rate. Similarly, in our work, we have selected a different class of two-qubit mixed entangled states, described by Eq. (4), to evaluate the key rate. In what follows, we demonstrate that a positive key rate can also be achieved with this class of mixed states, despite a small CHSH violation. We focus on this particular class of mixed states to compare the key rate obtained under the collective attack scenario with that derived in the sequential attack model, which we introduce in the subsequent section.

In this scenario, the CHSH value between Alice and Bob is given by

$$\mathcal{S}_{AB} = \frac{1}{\sqrt{2}} \left( 2 + \sqrt{1 - \alpha^2} \right) \quad (5)$$

For ensuring CHSH violation, the parameter  $\alpha$  is bounded by  $\alpha \in [0, \sqrt{8\sqrt{2} - 11} \approx 0.5601]$ . In this range, the CHSH value is constrained to the interval  $\mathcal{S}_{AB} \in (2, \frac{3}{\sqrt{2}} \approx 2.1213]$ . The QBER is evaluated as

$$Q = p(a \neq b | A_0, B_1, \tilde{\rho}) = \frac{1}{4} \left( 1 - \sqrt{1 - \alpha^2} \right) \quad (6)$$

The key rate is evaluated from Eq. (2) by employing Eqs. (5) and (6). The lower bound of the key rate, denoted by  $(r_C)$ , represents the minimum security threshold in the worst possible case. It is evaluated by taking the upper bound of  $\chi(B_1 : E)$ , expressed as a function of QBER and the CHSH value, as given by [13]

$$r_C(Q, \mathcal{S}) = 1 - H(Q) - H\left(\frac{1}{2} \left[ 1 + \sqrt{(\mathcal{S}_{AB}/2)^2 - 1} \right]\right) \quad (7)$$

Note that  $r_C(Q, \mathcal{S})$  is found to be a monotonic increasing function of the CHSH value, thereby establishing that an increase in nonlocality will result in an increasing lower bound of the key rate as illustrated by curve 'b' of Fig. 1. The lower bound of the key rate is non-zero, i.e.,  $r_C(Q, \mathcal{S}) \in (0, 0.0921]$  for  $Q \in [0, 0.0086]$  and  $\mathcal{S}_{AB} \in [2.0965, 2.1213]$ , implying  $\alpha \in (0, 0.2625]$ .

In the following analysis, we demonstrate that in addition to the conventional collective attack, Eve can gain more information if she carries out a sequential attack. In particular, we show that for an identical CHSH violation, the non-zero key rate under a standard collective attack can become zero when Eve's sequential attack is taken into account.

### III. DI-QKD UNDER SEQUENTIAL ATTACK

Let us first elaborately explain the sequential attack strategy and how, with such a strategy, Eve can get more information.

In this attack, Eve intercepts the qubit sent by Alice to Bob after preparing the maximally entangled state  $\rho = |\phi^+\rangle\langle\phi^+|$  during the transmission phase. In order

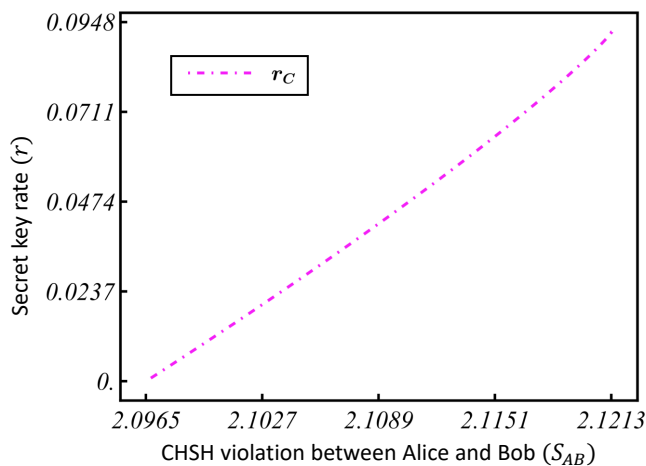


FIG. 1: Key rate ( $r$ ) as a function of the CHSH violation between Alice and Bob ( $S_{AB}$ ). The purple dashed-dotted is the key rate under a collective attack.

to mask her attack, Eve performs an unsharp measurement such that the CHSH violation between Alice and Bob remains the same as in Eq. (5). Intuitively, one might expect Eve’s measurement to disturb the state, preventing Alice and Bob from observing CHSH violations. However, recent results show that Bell nonlocality can be sequentially shared among Alice and multiple independent Bobs through simultaneous violations of the CHSH inequality [28–30, 32, 33]. Eve exploits this fact in her attack strategy to gain additional information about the shared key between Alice and Bob. This sequential attack strategy is depicted in Fig. 2.

### A. Proposed setup for the sequential attack strategy

The sequential attack can be realized using the setups employed in recent experimental demonstrations of the sequential sharing of nonlocal correlations [56, 57, 80]. This attack can be implemented with a straightforward optical experimental setup, as depicted in Fig. 2. The setup comprises the following four distinct stages:

(i) *Quantum state preparation.*— Entangled photon pairs are generated via spontaneous parametric down-conversion (SPDC) in nonlinear crystals, such as periodically poled lithium niobate (PPLN) or beta barium borate (BBO) crystals [81, 82]. Alice retains one photon from each pair and sends the other photon to Bob’s laboratory.

(ii) *Eve’s measurement set up.*— Eve employs von Neumann-type measurement frameworks [28, 83] to perform unsharp measurements on the photon directed to Bob’s lab. For an unsharp measurement in the direction ( $\sigma_\beta = |\beta\rangle\langle\beta| - |\beta_\perp\rangle\langle\beta_\perp|$ ), Eve performs an optical transformation. Measuring ( $\sigma_\beta$ ) involves rotating two half-wave plates (HWPs), (HWP1) and (HWP4), by ( $\frac{\beta}{2}$ ). A

Beam Displacer (BD) establishes weak coupling between the system and the pointer. The angles for (HWP2) and (HWP3) are set to ( $\frac{\phi}{2}$ ) and ( $\frac{\pi}{4} - \frac{\phi}{2}$ ), respectively. The quality factor  $F = \sin 2\phi$  enables ( $\phi$ ) to vary from ( $\frac{\pi}{4}$ ) to 0, transitioning from weak to strong coupling. Outcomes of +1 or –1 are determined by rotating (HWP1) and (HWP4) by ( $\frac{\beta}{2}$ ) or ( $\frac{\beta}{2} + \frac{\pi}{4}$ ), respectively, and, positioning optical shutters (OS) and beam displacers appropriately [57]. By this method, Eve performs the desired measurements: ( $\sigma_z$ ) with bias  $q$  by setting ( $\phi = 0$ ) (strong measurement,  $\gamma_1 = 1$ ), and ( $\gamma\sigma_x$ ) with bias  $1 - q$  by choosing ( $\phi = \phi_0$ ) (weak measurement,  $\gamma_2 = \gamma = \cos 2\phi$ ).

(iii) *Alice’s measurement.*— Alice selects her measurement basis randomly using a quantum random number generator and chooses one of the three measurements specified in Eq. (9). She then rotates her half-wave plate (HWP<sub>A</sub>) by angles of 0,  $\frac{\theta}{2}$  or  $\frac{\pi}{2} - \frac{\theta}{2}$ , corresponding to  $A_0$ ,  $A_1$  and  $A_2$ , respectively, where  $\theta$  is predetermined by Eve.

(iv) *Bob’s measurement.*— Bob also selects a measurement basis randomly and chooses one of the two measurements specified in Eq. (3). He then rotates his half-wave plate (HWP<sub>B</sub>) by an angle of 0 or  $\frac{\pi}{4}$ , corresponding to measurements of  $\sigma_z$  and  $\sigma_x$ , respectively.

After the photons pass through HWP<sub>A</sub> or HWP<sub>B</sub>, Alice and Bob perform strong measurements on their respective photons using a Polarising Beam Splitter (PBS) coupled with a detector.

It is to be noted that a quantum adversary’s setup possesses all the capabilities of Alice and Bob’s setups and may be further augmented by quantum computational capabilities. Such enhancement would enable the implementation of advanced and optimised versions of such attacks (see Fig. 2) in future scenarios.

### B. Sequential attack strategy

It may be emphasized here that since Alice uses  $A_0$  to establish the key with Bob, Eve’s optimal strategy is to measure  $E_1 = A_0$  consistently to maximise her mutual information with Alice. However, performing  $E_1 = A_0$  exclusively would completely destroy the state’s correlation, rendering it separable and preventing any CHSH violation between Alice and Bob. To avoid this, Eve performs unsharp measurements of  $E_1$  with probability  $q$  and  $E_2$  with probability  $1 - q$  with  $q > 1 - q$ . To optimise her mutual information, Eve maximises  $q$ , adjusts Alice’s other measurement directions ( $A_1, A_2$ ) by an angle  $\theta$ , and selects unsharp parameters  $\gamma_1, \gamma_2$  such that CHSH violation between Alice and Bob remains unchanged, as per Eq. (5). The unsharp measurement performed by Eve is characterized by [84]

$$M_e \equiv \left\{ \mathcal{E}_{g|e} = \frac{1}{2}(\mathbb{1} + \gamma_e E_e); e \in \{1, 2\} \right\} \quad (8)$$

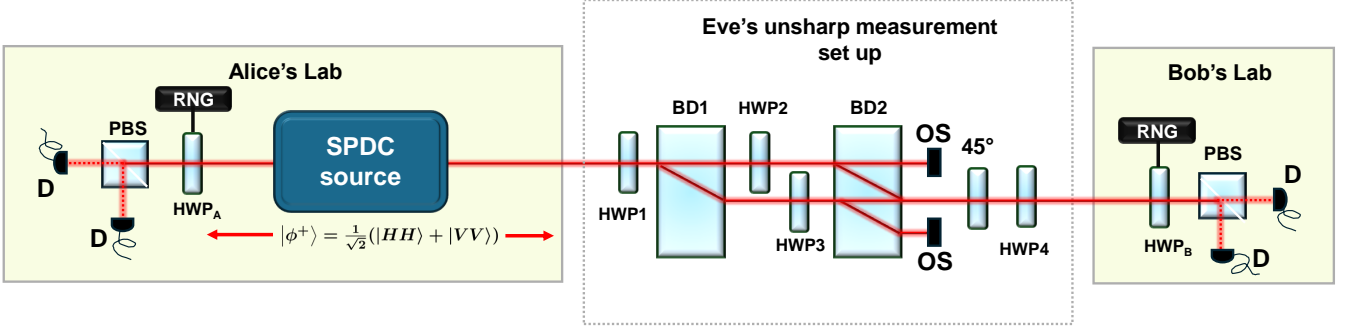


FIG. 2: Proposed setup for DI-QKD under sequential attack. Entangled photon pairs are generated via SPDC and sent to Alice and Bob. Eve performs unsharp measurements using a combination of Beam Displacers (BD), Half-Wave Plates (HWP) to simulate weak and strong measurements. Alice and Bob randomly select measurement settings, rotating their HWPs to measure in different bases, followed by detection through Polarising Beam Splitters (PBS) and detectors (D).

where  $E_1 = A_0 = \sigma_z$  and  $E_2 = \sigma_x$ ;  $g \in \{0, 1\}$ . Alice's rotated measurement directions ( $A_1, A_2$ ) are given by

$$A_1 = \cos \theta \sigma_z + \sin \theta \sigma_x; \quad A_2 = \cos \theta \sigma_z - \sin \theta \sigma_x \quad (9)$$

Next, Eve transfers the post-measurement qubit to Bob. During the device-independence test, when Alice publishes her outcome, Eve collects Alice's outcome statistics and evaluates the joint probability distribution as  $p(a, g|A_x, M_e) = \text{Tr}[\rho A_{a|x} \otimes \mathcal{E}_{g|e}]$ . As a result of Eve's unsharp measurement in a biased input manner, the state evolves into a mixed entangled two-qubit state,  $\rho_1$ , as described by Luder's transformation rule [84]. Since Eve performs two distinct measurements on  $\rho$ , the post-measurement states are produced with probabilities  $q$  and  $1 - q$ , and are given by

$$(\rho)_{M_e} \rightarrow \sum_g \left( \mathbb{I} \otimes \sqrt{\mathcal{E}_{g|e}} \right) \rho \left( \mathbb{I} \otimes \sqrt{\mathcal{E}_{g|e}} \right) \quad (10)$$

Since Bob doesn't have any information about Eve's unsharp measurement, the post-measurement state  $\rho_1$  after Eve's measurement is

$$\rho_1 = q (\rho)_{M_1} + (1 - q) (\rho)_{M_2} \quad (11)$$

To evaluate the quantity  $\sqrt{\mathcal{E}_{g|e}}$  in Eq. (10), we take recourse to the Kraus-operator formalism [84]. The Kraus operators are given by

$$\mathbf{K}_e \equiv \left\{ \mathcal{K}_{g|e} \left| \mathcal{K}_{g|e}^\dagger \mathcal{K}_{g|e} \geq 0, \sum_g \mathcal{K}_{g|e}^\dagger \mathcal{K}_{g|e} = \mathbb{I} \right. \right\} \quad (12)$$

We construct Kraus operator such a way, so that  $(\mathcal{K}_{g|e})^\dagger (\mathcal{K}_{g|e}) = \mathcal{E}_{g|e}$  and, in turn,  $\sqrt{\mathcal{E}_{g|e}} = \mathcal{K}_{g|e}$ . The Kraus operator in this scenario is then given as follows

$$\mathcal{K}_{g|e} = K_0 \mathbb{I} + (-1)^g K_1 E_e \quad (13)$$

where  $K_i = \frac{\sqrt{1+\gamma_e} + (-1)^i \sqrt{1-\gamma_e}}{2\sqrt{2}}$  with  $i \in \{0, 1\}$ . The average reduced state after Eve's unsharp measurement given

by Eq. (11) is evaluated as

$$\begin{aligned} \rho_1 &= \sum_e \sum_g q_e (\mathbb{I} \otimes \mathcal{K}_{g|e}) \rho (\mathbb{I} \otimes \mathcal{K}_{g|e}) \\ &= \frac{1}{2} \left[ 1 + q \sqrt{1 - \gamma_1^2} + (1 - q) \sqrt{1 - \gamma_2^2} \right] |\Phi^+\rangle \langle \Phi^+| \\ &\quad + \frac{q}{2} \left( 1 - \sqrt{1 - \gamma_1^2} \right) |\Phi^-\rangle \langle \Phi^-| \\ &\quad + \frac{1 - q}{2} \left( 1 - \sqrt{1 - \gamma_2^2} \right) |\Psi^+\rangle \langle \Psi^+| \end{aligned} \quad (14)$$

Note that with these choices of measurements by Eve and Alice, the nonlocality between them will be ensured by the violation of a biased Bell inequality. The biased Bell inequality [85] where one party measures in an unbiased manner and the other party measures with an input bias  $q \geq \frac{1}{2}$  is expressed as

$$\begin{aligned} \mathcal{S}_{Biased} &= \frac{q}{2} [\langle A_0 B_0 \rangle - \langle A_0 B_1 \rangle + \langle A_1 B_0 \rangle + \langle A_1 B_1 \rangle] \\ &\quad + \frac{1}{2} (\langle A_0 B_1 \rangle + \langle A_1 B_1 \rangle) - \langle A_1 B_1 \rangle \leq q \end{aligned} \quad (15)$$

The corresponding nonlocality between Alice and Eve is given by

$$\mathcal{S}_{AE} = \gamma_1 q \cos \theta + \gamma_2 (1 - q) \sin \theta \quad (16)$$

Nonlocality between Alice and Eve is ensured for the following conditions

$$\begin{cases} \gamma_1 \cos \theta - \gamma_2 \sin \theta > 1 & \text{if } \frac{1}{2} \leq q \leq 1 \\ \gamma_1 \cos \theta - \gamma_2 \sin \theta < 1 & \text{if } \frac{1}{2} \leq q < \frac{\gamma_2 \sin \theta}{\gamma_1 \cos \theta - \gamma_2 \sin \theta - 1} \end{cases}$$

For the reduced state  $\rho_1$ , the CHSH value between Alice and Bob is

$$\begin{aligned} \mathcal{S}'_{AB} &= 2 \left[ \sin \theta - q \sin \theta \left( 1 - \sqrt{1 - \gamma_1^2} \right) \right. \\ &\quad \left. + \cos \theta \left( q + \sqrt{1 - \gamma_2^2} - q \sqrt{1 - \gamma_2^2} \right) \right] \end{aligned} \quad (17)$$

It needs to be mentioned that even if Eve chooses her first measurement,  $E_1 = A_0$ , to maximise the information gain, the CHSH value between Alice and Bob persists. In this case, for  $\gamma_1 = 1$ , the CHSH value between Alice and Bob reduces to the following expression (writing  $\gamma_2 = \gamma$  from now on)

$$\mathcal{S}'_{AB} = 2 \left[ q \cos \theta + (1 - q) \left( \sin \theta + \cos \theta \sqrt{1 - \gamma^2} \right) \right] \quad (18)$$

Both Bob and Eve demonstrate simultaneous nonlocality with Alice under the following conditions

$$\frac{q \tan \frac{\theta}{2}}{1 - q} < \gamma < \sqrt{1 - \left[ \frac{1 - \sin \theta - \sqrt{2}q \sin(\frac{\pi}{4} - \theta)}{(1 - q) \cos \theta} \right]^2} \quad (19)$$

Note that  $\gamma \in (0, 1)$  will always exist if the lower and upper bounds of  $\gamma$ , denoted by  $\gamma_l$  and  $\gamma_u$ , respectively, also lie within the range  $(0, 1)$ . These constraints establish the upper bound of the bias parameter  $q$ . Given  $\gamma_l \in (0, 1)$  and  $q > 1 - q$ , we obtain

$$\frac{1}{2} \leq q < \frac{1}{1 + \tan \frac{\theta}{2}} \quad (20)$$

Similarly, the condition  $\gamma_u \in (0, 1)$  implies

$$\frac{1}{2} \leq q < 1 - \tan \frac{\theta}{2} \quad (21)$$

Since the upper bound of  $q$  in Eq. (20) is greater than that in Eq. (21) for any  $\theta \in (0, \frac{\pi}{4})$ , we can, without loss of generality, restrict the permissible range of  $q$  in accordance with the bound provided by Eq. (21). Thus, there exist specific ranges of  $q \in [\frac{1}{2}, 1 - \tan \frac{\theta}{2}]$ ,  $\gamma \in (\gamma_l, \gamma_u)$  and  $\theta \in (0, \frac{\pi}{4})$  for which both Bob and Eve demonstrate nonlocality with Alice.

### C. Evaluation of the key rate under sequential attack

The crux of the sequential attack strategy hinges on Eve's ability to emulate the observed CHSH violation between Alice and Bob (without a sequential attack) by precisely adjusting the unsharpness parameters  $\gamma$ , biasness parameter  $q$ , and Alice's fabricated measurement settings  $\theta$  such that  $\mathcal{S}_{AB}(\alpha) = \mathcal{S}'_{AB}(q, \gamma, \theta)$ . In this process, Eve can augment the accessible information by aligning  $E_1$  with  $A_0$  and generating nonlocal correlations by accessing the shared state  $\rho$  through the violation of a biased input Bell inequality [85], thereby enabling an individual attack. The impact of this attack is reflected in the following evaluation of the lower bound of the key rate.

This sequential measurement strategy is an individual attack, as Eve independently intercepts each system sent from Alice to Bob, applying the same method consistently. Eve measures her ancilla before classical post-processing without having access to any quantum memory. As a result, Eve, Alice, and Bob share a product distribution of classical symbols [76].

To evaluate the lower bound of the key rate, denoted by  $r_S$ , we first evaluate the modified QBER as follows,

$$Q^S = p(a \neq b | A_0, B_1, \rho_1) = \frac{1 - q}{2} \left( 1 - \sqrt{1 - \gamma^2} \right) \quad (22)$$

In the context of a sequential attack, the lower bound of the key rate is given by [86],

$$\begin{aligned} r_S &= \mathcal{I}(A_0 : B_1) - [q\mathcal{I}(A_0 : E_1) + (1 - q)\mathcal{I}(A_0 : E_2)] \\ &= 1 - H(Q^S) - q \end{aligned} \quad (23)$$

To compare the new key rate resulting from this individual sequential attack in Eq. (23) with that obtained under collective attack by Eq. (7), we require stricter bounds for the bias parameter ( $q$ ), Alice's measurement angle ( $\theta$ ) and the unsharp parameter ( $\gamma$ ) for ensuring same CHSH violation obtained by Eq. (5), i.e.  $\mathcal{S}_{AB} \in (2, 2.1213]$ . Thus, using the bounds provided in the para below Eq. (7), and setting  $\mathcal{S}'_{AB} = \mathcal{S}_{AB} \in [2.0965, 2.1213]$  leads to the following condition (see Appx. A),

$$\gamma_{nl} < \gamma < \gamma_{nu} \quad (24)$$

The expressions for  $\gamma_{nl}$  and  $\gamma_{nu}$  are provided in Eq. (A2) of Appx. A. We find that the condition  $\gamma_{nl}, \gamma_{nu} \in (0, 1)$  leads to the following set of restrictions on the bias parameter  $q$  and the measurement angle  $\theta$  as follows.

$$\frac{1}{2} \leq q < q_{u1} \quad \forall \theta \in [0.1420, \frac{\pi}{4}] \quad (25)$$

$$\frac{1}{2} \leq q < q_{u2} \quad \forall \theta \in [0.1025, \frac{\pi}{4}] \quad (26)$$

The expressions for  $q_{u1}$  and  $q_{u2}$  are given by Eqs. (A4) and (A5) of Appx. A. Without loss of generality, these expressions are evaluated under the assumptions  $q > 1 - q$ . Since  $q_{u2} > q_{u1}$  for  $\theta \in [0.1420, \frac{\pi}{4}]$  (see Fig. 3), we can, without loss of generality, consider the permissible range of  $q$  as determined by the bound in Eq. (25).

To maintain the QBER as given by Eq. (22), within the acceptable range of  $[0, 0.0086]$ , we derive a new upper bound of  $\gamma$

$$0 < \gamma < \gamma_{nu1} \quad (27)$$

The expression for  $\gamma_{nu1}$  is given by Eq. (A6) of Appx. A. Furthermore, for  $\gamma_{nu1}$  to be a valid bound, it must satisfy  $\gamma_{nl} \leq \gamma_{nu1} \leq \gamma_{nu}$ . This condition results in four regions for  $\theta$  and  $q$  (See Appx. A). Among these, a specific region (Region 2, illustrated by the sky-blue zone in Fig. 3) provides the strict upper and lower bounds of both  $q$  and  $\theta$ , as given by

$$q_l \leq q < q_{u3} ; \text{ and } \theta \in [0.1927, 0.7456] \quad (28)$$

It may be reemphasized that the bounds on  $q$  and  $\theta$ , specified by Eq. (28), ensure the observed CHSH violation lies within  $[2.0965, 2.1213]$ , while the QBER remains in the range  $[0, 0.0086]$ .

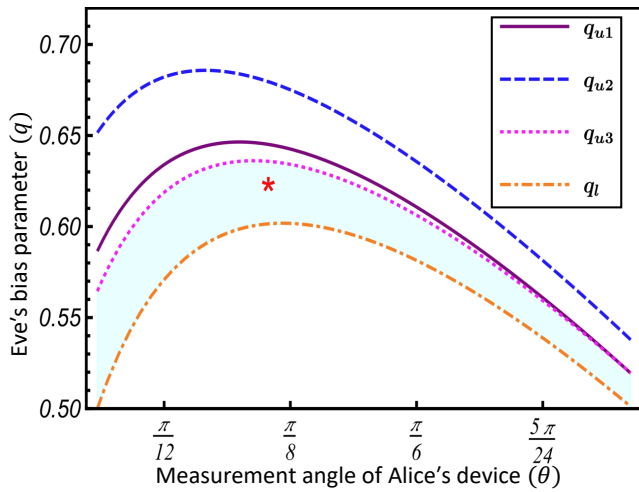


FIG. 3: Bounds of Eve’s bias parameter ( $q$ ) as a function of Alice’s measurement angle ( $\theta$ ). The blue dashed, purple solid, magenta dotted, and orange dash-dotted lines represent  $q_{u1}$ ,  $q_{u2}$ ,  $q_{u3}$ , and  $q_l$ , respectively. The shaded region represents the considered CHSH violations and QBER range. The red point denotes an example with (\*)  $q^* = 0.625$  and  $\theta^* = 0.37$ .

Eve can select the upper bound of the bias parameter derived in Eq. (28), i.e.,  $q_{u3}$  to maximize her mutual information with Alice. For this choice of bias parameter and the allowed range of Alice’s measurement settings  $\theta$ , we find a region of the key rate corresponding to the CHSH violation  $S'_{AB} \in [2.0965, 2.1213]$ , as illustrated by region ‘a’ in Fig. 4. The lower bound of the key rate is represented by the red curve ‘b’ in Fig. 4. This lower bound is achieved when the bias parameter  $q$  attains its maximum value, i.e.,  $q_{um} = 0.6361$  with  $\theta_{um} = 0.3544$ . The lower bound of the key rate, ranging from  $[0.2936, 0.3444]$  bits, is found to be monotonically increasing with the CHSH violation,  $S'_{AB} \in [2.0965, 2.1213]$ . As illustrated, the key rate for the sequential attack consistently exceeds that of the collective attack (dashed curve ‘c’) for the same CHSH violation, remaining within the permissible range of QBER.

This result is expected because, in comparing individual and collective attacks, the collective attack is more powerful due to Eve’s access to quantum memory, allowing her to store her ancilla and perform a collective measurement later to extract more information [76]. In the following section, we will discuss the cumulative effect of both sequential and collective attacks.

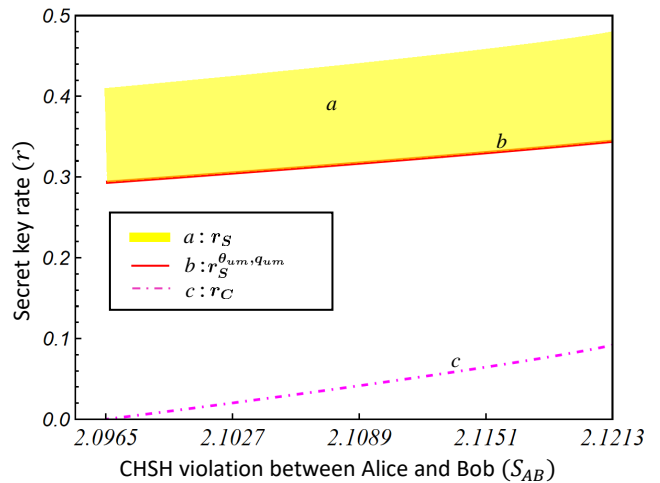


FIG. 4: Key rate ( $r$ ) as a function of the CHSH violation between Alice and Bob ( $S_{AB}$ ). The yellow region ‘a’ shows the key rate under a sequential attack ( $r_S$ ), the red curve ‘b’ represents its lower bound, and the purple dashed-dotted curve ‘c’ is the key rate under a collective attack.

#### IV. DI-QKD UNDER THE CUMULATIVE EFFECT OF SEQUENTIAL AND COLLECTIVE ATTACKS

In a standard collective attack scenario, Eve controls the preparation device, sending Alice and Bob a mixed two-qubit entangled state while retaining the purification qubit as an ancilla. Over multiple rounds, if Eve has access to a quantum memory, she can store these ancilla states and later perform collective measurements to extract information about the shared statistics between Alice and Bob.

In the scenario considered here, however, Alice prepares the bipartite state, thereby removing Eve’s control over the preparation device. Instead of retaining the purification as an ancilla, Eve intercepts the qubit sent from Alice to Bob, performs measurements following the strategy outlined in Sec. III B, and prepares an ancilla state based on the measurement outcomes. With access to quantum memory, Eve can store these ancilla states and subsequently perform collective measurements. This hybrid strategy combines elements of both sequential and collective attacks, requiring the key rate to be evaluated under their combined influence.

The effect of the collective attack [76] is captured by the extractable information,  $\chi(\mathcal{S}_{AB})$ , as given by Eq. (7), while the effect of the sequential attack is reflected in the error rate, QBER. The QBER depends on Eve’s control parameters  $q$ ,  $\gamma$  and  $\theta$ , as given in Eq. (22).

We demonstrate that combining these attacks results in a lower key rate compared to evaluating the scenario under a collective attack alone, within the permissible range of fluctuating QBER. Note that this feature is cap-

tured by evaluating the key rate using Eq. (7), with the CHSH violation  $\mathcal{S}_{AB}$  now being  $\mathcal{S}'_{AB}$ , which depends on Eve's control parameters  $\gamma$ ,  $\theta$  and  $q$ . In this context, the lower bound of the key rate is expressed as

$$r_{CS} = 1 - H(Q^S) - H\left(\frac{1}{2}\left[1 + \sqrt{(\mathcal{S}'_{AB}/2)^2 - 1}\right]\right) \quad (29)$$

We find the specific ranges for the parameters  $\gamma$ ,  $q$ , and  $\theta$  such that, for a given CHSH violation, the key rate evaluated by considering both sequential and collective attacks can become zero, even when the key rate under the Collective attack alone remains non-zero for the same CHSH violation. These parameter ranges include  $\gamma_{nl} \leq \gamma \leq \gamma_{nu1}$ ,  $q_l \leq q < q_{u3}$ , and  $\theta \in [0.1927, 0.7456]$ , as detailed in Sec. III C. We evaluate the secret key rate as a function of the CHSH violations for three suitably selected values of  $\theta$ : (i)  $\theta = \theta_{um} = 0.3544$ , corresponding to the maximum upper bound of the bias parameter ( $q_{um} = 0.6361$ ), (ii)  $\theta = \theta^* = 0.3700$ , an arbitrarily chosen angle with  $q = 0.6250$ , and (iii)  $\theta = \theta_{lm} = 0.3848$ , corresponding to the maximum lower bound of the bias parameter ( $q_{lm} = 0.6018$ ). The resulting variations in key rates with CHSH violations are illustrated in Fig. 5 as curves 'b', 'c', and 'd', respectively.

Furthermore, we identify a range of Eve's bias parameter,  $q \in [0.6018, 0.6361]$ , where she can select a specific value of  $\theta \in [0.1927, 0.7456]$  from the shaded region in Fig. 3 to ensure that the expected key rate between Alice and Bob under the combined sequential and collective attacks consistently remains lower than that under the collective attack alone, i.e.,  $r_{CS} < r_C$ , within the permissible range of fluctuating QBER,  $Q \in [0, 0.0086]$ . This behaviour is evident from curves 'b', 'c' and 'd' in Fig. 5, which all lie below the key rate observed under a collective attack, represented by the curve 'a'. Hence, we identify a region of CHSH violations where, despite  $r_C > 0$ , the combined attack reduces the key rate to zero, highlighting that CHSH violation alone is insufficient to ensure the security of DI-QKD.

In our analysis, the CHSH violation is notably low, which raises questions regarding its relevance in the context of DI-QKD. Nevertheless, recent studies demonstrate that DI-QKD remains feasible even with minimal non-locality [20]. Additionally, experimental findings confirm that the CHSH violation threshold aligns with the conditions considered in our case [80].

## V. SALIENT FEATURES AND OUTLOOK

With the advancement of loophole-free Bell experiments, DI-QKD is approaching practical implementation. However, real-world experiments are invariably subject to unavoidable noise and device imperfections, necessitating a comprehensive analysis of DI-QKD security under such conditions. Noise creates opportunities for adversarial interference, allowing Eve to exploit the

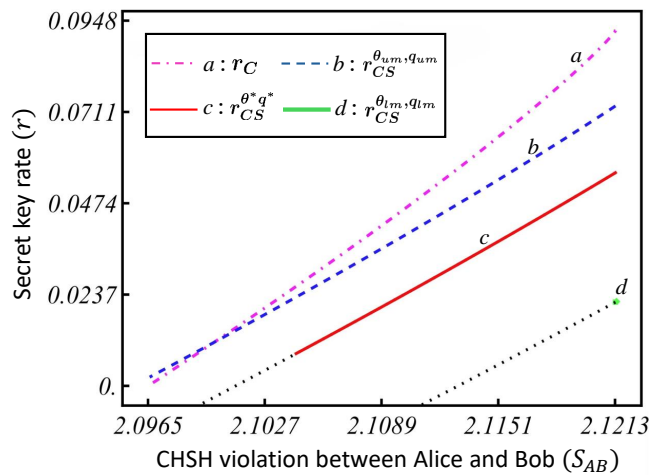


FIG. 5: Key rate ( $r$ ) as a function of the CHSH violation between Alice and Bob ( $\mathcal{S}_{AB}$ ). The purple dash-dotted curve 'a' represents the key rate under a collective attack ( $r_C$ ), while the blue dashed curve 'b' corresponds to a sequential collective attack ( $r_{CS}$ ) with Eve's parameters  $\theta_{um}$  and  $q_{um}$ . The red solid curve 'c' highlights a specific point within the shaded region in Fig. 3 (marked by a red '\*'), while the green dotted curve 'd' depicts the key rate for Eve's control parameters ( $\theta^*$ ,  $q^*$ ) and ( $\theta_{um}$ ,  $q_{um}$ ), respectively. The black dotted lines indicate where the QBER exceeds the threshold value of 0.0086.

expected non-maximal violation of a Bell inequality, effectively 'hiding behind the noise' to disguise her attacks.

In most DI-QKD scenarios, Eve is typically assumed to have control over both the entangled source and measurement devices. In our work, we consider a practical setting common in experimental or commercial DI-QKD, where the entangled source resides at Alice's node. To maintain the DI paradigm, we assume Eve can tamper with Alice's measurement device during manufacturing but lacks direct control over the source.

The central question we investigate is whether Eve can still execute a strong attack under this assumption. This does not undermine the principles of device independence, as the focus remains on mitigating attacks where Eve has partial control rather than full control over the system. While Jordan's lemma implies that the state shared between Alice and Bob could be expressed as a classical mixture of Bell states, our framework explores a specific practical scenario where Eve's indirect influence through sequential attacks is the primary concern. This assumption is necessary to reflect the realistic constraints of certain DI-QKD implementations and highlights vulnerabilities that persist even under these conditions.

Our study demonstrates that Eve can intercept a qubit sent from Alice to Bob, perform unsharp measurements, and prepare an ancillary state based on her measurement outcomes. The resulting post-measurement mixed state retains a non-maximal violation of the CHSH inequality,



which Alice and Bob may mistakenly attribute to noise in the quantum channel. Furthermore, Eve can mask her interference by controlling Alice’s measurement angles. By using quantum memory, she can store ancillary states and later perform collective measurements to extract information.

By extending the framework for key rate estimation to incorporate both sequential and collective attacks, we have shown how Eve can optimise her control parameters, such as the bias parameter, unsharpness parameter, and measurement angle, to maximise information extraction while preserving the appearance of security. Notably, the combination of sequential and collective attacks poses a significantly greater threat to DI-QKD security than either attack alone. Within a narrow range of fluctuating QBER, we have identified parameter regimes where the cumulative effect of these attacks renders the key rate zero, even when a collective attack alone would result in a non-zero key rate. This underscores the critical importance of addressing sequential attacks in the presence of unavoidable noise and device imperfections, as these attacks exploit the expected reduction in CHSH violations without raising suspicion.

Our findings reveal that the CHSH violation alone is insufficient to guarantee security against advanced attacks. To ensure robust DI-QKD, it is essential to develop noise-resilient protocols and security proofs that explicitly account for unsharp measurements and sequential interference. Experimental verification of these attacks in real-

world quantum communication setups will be crucial to assess their practical feasibility and refine existing protocols. Additionally, extending theoretical analyses to derive tighter security bounds against combined attack strategies, including sequential and coherent attacks, can further strengthen DI-QKD guarantees.

While all entangled states exhibit nonlocality [9], recent findings suggest that nonlocality alone may not suffice for DI-QKD security in classical-input Bell scenario. This raises a critical question: could all entangled states be suitable for DI-QKD in the quantum-input Bell scenario? Furthermore, it would be valuable to explore whether the security bound derived for combined sequential and collective attacks remain valid against the most general (coherent) attacks [87, 88].

This work emphasises the need to re-evaluate foundational assumptions in DI-QKD, integrating theoretical advancements with experimental validations. Addressing these challenges is vital to ensure robust and secure quantum communication in the presence of realistic noise and adversarial interference.

## VI. ACKNOWLEDGEMENTS

S.S. acknowledges support by the National Natural Science Fund of China (Grant No. G0512250610191). S. G. acknowledges OIST, Japan for the postdoctoral fellowship.

- 
- [1] C. E. Shannon, Communication theory of secrecy systems, *The Bell System Technical Journal* **28**, 656 (1949).
- [2] C. Portmann and R. Renner, Security in quantum cryptography, *Rev. Mod. Phys.* **94**, 025008 (2022).
- [3] A. Acín, S. Massar, and S. Pironio, Efficient quantum key distribution secure against no-signalling eavesdroppers, *New Journal of Physics* **8**, 126–126 (2006).
- [4] A. Acín, N. Gisin, and L. Masanes, From bell’s theorem to secure quantum key distribution, *Phys. Rev. Lett.* **97**, 120405 (2006).
- [5] A. Ekert and R. Renner, The ultimate physical limits of privacy, *Nature* **507**, 443 (2014).
- [6] N. Brunner, D. Cavalcanti, S. Pironio, V. Scarani, and S. Wehner, Bell nonlocality, *Rev. Mod. Phys.* **86**, 419 (2014).
- [7] J. S. Bell, On the einstein podolsky rosen paradox, *Physics Physique Fizika* **1**, 195 (1964).
- [8] J. S. BELL, On the problem of hidden variables in quantum mechanics, *Rev. Mod. Phys.* **38**, 447 (1966).
- [9] F. Buscemi, All entangled quantum states are nonlocal, *Phys. Rev. Lett.* **108**, 200401 (2012).
- [10] D. Schmid, T. C. Fraser, R. Kunjwal, A. B. Sainz, E. Wolfe, and R. W. Spekkens, Understanding the interplay of entanglement and nonlocality: motivating and developing a new branch of entanglement theory, *Quantum* **7**, 1194 (2023).
- [11] E. G. Cavalcanti and H. M. Wiseman, Bell nonlocality, signal locality and unpredictability (or what bohr could have told einstein at solvay had he known about bell experiments), *Foundations of Physics* **42**, 1329 (2012).
- [12] I. Devetak and A. Winter, Distillation of secret key and entanglement from quantum states, *Proceedings of the Royal Society A: Mathematical, Physical and Engineering Sciences* **461**, 207–235 (2005).
- [13] A. Acín, N. Brunner, N. Gisin, S. Massar, S. Pironio, and V. Scarani, Device-independent security of quantum cryptography against collective attacks, *Phys. Rev. Lett.* **98**, 230501 (2007).
- [14] U. Vazirani and T. Vidick, Fully device-independent quantum key distribution, *Phys. Rev. Lett.* **113**, 140501 (2014).
- [15] R. Arnon-Friedman, F. Dupuis, O. Fawzi, R. Renner, and T. Vidick, Practical device-independent quantum cryptography via entropy accumulation, *Nature Communications* **9**, 459 (2018).
- [16] S. Pirandola, U. L. Andersen, L. Banchi, M. Berta, D. Bunandar, R. Colbeck, D. Englund, T. Gehring, C. Lupo, C. Ottaviani, J. L. Pereira, M. Razavi, J. Shamsul Shaari, M. Tomamichel, V. C. Usenko, G. Vallone, P. Villoresi, and P. Wallden, Advances in quantum cryptography, *Advances in Optics and Photonics* **12**, 1012 (2020).
- [17] P. Sekatski, J.-D. Bancal, X. Valcarce, E. Y.-Z. Tan, R. Renner, and N. Sangouard, Device-independent quantum key distribution from generalized CHSH inequalities, *Quantum* **5**, 444 (2021).

- [18] R. Schwonnek, K. T. Goh, I. W. Primaatmaja, E. Y.-Z. Tan, R. Wolf, V. Scarani, and C. C.-W. Lim, Device-independent quantum key distribution with random key basis, *Nature communications* **12**, 2880 (2021).
- [19] V. Zapatero, T. van Leent, R. Arnon-Friedman, W.-Z. Liu, Q. Zhang, H. Weinfurter, and M. Curty, Advances in device-independent quantum key distribution, *npj quantum information* **9**, 10 (2023).
- [20] L. Woollorton, P. Brown, and R. Colbeck, Device-independent quantum key distribution with arbitrarily small nonlocality, *Phys. Rev. Lett.* **132**, 210802 (2024).
- [21] M. Farkas, Unbounded device-independent quantum key rates from arbitrarily small nonlocality, *Phys. Rev. Lett.* **132**, 210803 (2024).
- [22] A. K. Ekert, B. Huttner, G. M. Palma, and A. Peres, Eavesdropping on quantum-cryptographical systems, *Physical Review A* **50**, 1047–1056 (1994).
- [23] B. A. Slutsky, R. Rao, P.-C. Sun, and Y. Fainman, Security of quantum cryptography against individual attacks, *Physical Review A* **57**, 2383–2398 (1998).
- [24] N. Lütkenhaus, Estimates for practical quantum cryptography, *Physical Review A* **59**, 3301–3319 (1999).
- [25] S. Pironio, A. Acín, N. Brunner, N. Gisin, S. Massar, and V. Scarani, Device-independent quantum key distribution secure against collective attacks, *New Journal of Physics* **11**, 045021 (2009).
- [26] P. W. Shor and J. Preskill, Simple proof of security of the bb84 quantum key distribution protocol, *Physical Review Letters* **85**, 441–444 (2000).
- [27] J. F. Clauser, M. A. Horne, A. Shimony, and R. A. Holt, Proposed experiment to test local hidden-variable theories, *Physical Review Letters* **23**, 880–884 (1969).
- [28] R. Silva, N. Gisin, Y. Guryanova, and S. Popescu, Multiple observers can share the nonlocality of half of an entangled pair by using optimal weak measurements, *Phys. Rev. Lett.* **114**, 250401 (2015).
- [29] S. Mal, A. S. Majumdar, and D. Home, Sharing of nonlocality of a single member of an entangled pair of qubits is not possible by more than two unbiased observers on the other wing, *Mathematics* **4**, 48 (2016).
- [30] P. J. Brown and R. Colbeck, Arbitrarily many independent observers can share the nonlocality of a single maximally entangled qubit pair, *Phys. Rev. Lett.* **125**, 090401 (2020).
- [31] A. Steffnlongo and A. Tavakoli, Projective measurements are sufficient for recycling nonlocality, *Phys. Rev. Lett.* **129**, 230402 (2022).
- [32] S. Sasmal, S. Kanjilal, and A. K. Pan, Unbounded sharing of nonlocality using qubit projective measurements, *Phys. Rev. Lett.* **133**, 170201 (2024).
- [33] Z. Cai, C. Ren, T. Feng, X. Zhou, and J. Chen, A review of quantum correlation sharing: The recycling of quantum correlations triggered by quantum measurements, *Physics Reports* **1098**, 1 (2024).
- [34] G. Foletto, L. Calderaro, A. Tavakoli, M. Schiavon, F. Picciariello, A. Cabello, P. Villoresi, and G. Vallone, Experimental certification of sustained entanglement and nonlocality after sequential measurements, *Phys. Rev. Appl.* **13**, 044008 (2020).
- [35] M. Pandit, C. Srivastava, and U. Sen, Recycled entanglement detection by arbitrarily many sequential and independent pairs of observers, *Phys. Rev. A* **106**, 032419 (2022).
- [36] A. K. Das, D. Das, S. Mal, D. Home, and A. S. Majumdar, Resource-theoretic efficacy of the single copy of a two-qubit entangled state in a sequential network, *Quantum Information Processing* **21**, 381 (2022).
- [37] M.-L. Hu and H. Fan, Sequential sharing of two-qubit entanglement based on the entropic uncertainty relation, *Phys. Rev. A* **108**, 012423 (2023).
- [38] S. Sasmal, D. Das, S. Mal, and A. S. Majumdar, Steering a single system sequentially by multiple observers, *Phys. Rev. A* **98**, 012305 (2018).
- [39] A. Shenoy H., S. Designolle, F. Hirsch, R. Silva, N. Gisin, and N. Brunner, Unbounded sequence of observers exhibiting einstein-podolsky-rosen steering, *Phys. Rev. A* **99**, 022317 (2019).
- [40] X.-H. Han, T. Qian, S.-C. Dong, S. Wang, Y. Xiao, and Y.-J. Gu, Activation of einstein-podolsky-rosen steering sharing with unsharp nonlocal measurements, *Scientific Reports* **14**, 11462 (2024).
- [41] J. Zhu, M.-J. Hu, C.-F. Li, G.-C. Guo, and Y.-S. Zhang, Einstein-podolsky-rosen steering in two-sided sequential measurements with one entangled pair, *Phys. Rev. A* **105**, 032211 (2022).
- [42] Y. X. Rong, S. Wang, Z. F. Zhang, Y. J. Gu, and Y. Xiao, Sharing asymmetric einstein-podolsky-rosen steering with projective measurements, *New Journal of Physics* **26**, 083014 (2024).
- [43] D. Das, A. Ghosal, S. Sasmal, S. Mal, and A. S. Majumdar, Facets of bipartite nonlocality sharing by multiple observers via sequential measurements, *Phys. Rev. A* **99**, 022305 (2019).
- [44] S. S. Mahato and A. K. Pan, Sharing nonlocality in a quantum network by unbounded sequential observers, *Phys. Rev. A* **106**, 042218 (2022).
- [45] J.-H. Wang, Y.-J. Wang, L.-J. Wang, and Q. Chen, Network nonlocality sharing via weak measurements in the generalized star network configuration, *Phys. Rev. A* **106**, 052412 (2022).
- [46] Y.-L. Mao, Z.-D. Li, A. Steffnlongo, B. Guo, B. Liu, S. Xu, N. Gisin, A. Tavakoli, and J. Fan, Recycling nonlocality in quantum star networks, *Phys. Rev. Res.* **5**, 013104 (2023).
- [47] H. Sun, F. Guo, H. Dong, and F. Gao, Network nonlocality sharing in a two-forked tree-shaped network, *Phys. Rev. A* **110**, 012401 (2024).
- [48] S. Datta and A. S. Majumdar, Sharing of nonlocal advantage of quantum coherence by sequential observers, *Phys. Rev. A* **98**, 042311 (2018).
- [49] A. Kumari and A. K. Pan, Sharing nonlocality and non-trivial preparation contextuality using the same family of bell expressions, *Phys. Rev. A* **100**, 062130 (2019).
- [50] A. Kumari and A. K. Pan, Sharing preparation contextuality in a bell experiment by an arbitrary pair of sequential observers, *Phys. Rev. A* **107**, 012615 (2023).
- [51] S. Saha, D. Das, S. Sasmal, D. Sarkar, K. Mukherjee, A. Roy, and S. S. Bhattacharya, Sharing of tripartite nonlocality by multiple observers measuring sequentially at one side, *Quantum Information Processing* **18**, 42 (2019).
- [52] A. G. Maity, D. Das, A. Ghosal, A. Roy, and A. S. Majumdar, Detection of genuine tripartite entanglement by multiple sequential observers, *Phys. Rev. A* **101**, 042340 (2020).
- [53] S. Gupta, A. G. Maity, D. Das, A. Roy, and A. S. Majumdar, Genuine einstein-podolsky-rosen steering of three-qubit states by multiple sequential observers, *Phys. Rev.*

- A **103**, 022421 (2021).
- [54] Y. Xi, M.-S. Li, L. Fu, and Z.-J. Zheng, Sharing tripartite nonlocality sequentially by arbitrarily many independent observers, *Phys. Rev. A* **107**, 062419 (2023).
- [55] T. Zhang, H. Yang, and S.-M. Fei, Sharing bell nonlocality of bipartite high-dimensional pure states using only projective measurements, *Phys. Rev. A* **109**, 022419 (2024).
- [56] M. Schiavon, L. Calderaro, M. Pittaluga, G. Vallone, and P. Villoresi, Three-observer bell inequality violation on a two-qubit entangled state, *Quantum Science and Technology* **2**, 015010 (2017).
- [57] M.-J. Hu, Z.-Y. Zhou, X.-M. Hu, C.-F. Li, G.-C. Guo, and Y.-S. Zhang, Observation of non-locality sharing among three observers with one entangled pair via optimal weak measurement, *npj Quantum Information* **4**, 63 (2018).
- [58] T. Feng, C. Ren, Y. Tian, M. Luo, H. Shi, J. Chen, and X. Zhou, Observation of nonlocality sharing via not-so-weak measurements, *Phys. Rev. A* **102**, 032220 (2020).
- [59] Y. Xiao, Y. X. Rong, S. Wang, X. H. Han, J. S. Xu, and Y. J. Gu, Experimental sharing of bell nonlocality with projective measurements, *New Journal of Physics* **26**, 053019 (2024).
- [60] S. Virzì, E. Rebuffello, F. Atzori, A. Avella, F. Piacentini, R. Lussana, I. Cusini, F. Madonini, F. Villa, M. Gramegna, E. Cohen, I. P. Degiovanni, and M. Genovese, Entanglement-preserving measurement of the bell parameter on a single entangled pair, *Quantum Science and Technology* **9**, 045027 (2024).
- [61] F. J. Curchod, M. Johansson, R. Augusiak, M. J. Hoban, P. Wittek, and A. Acín, Unbounded randomness certification using sequences of measurements, *Phys. Rev. A* **95**, 020102 (2017).
- [62] G. Foletto, M. Padovan, M. Avesani, H. Tebyanian, P. Villoresi, and G. Vallone, Experimental test of sequential weak measurements for certified quantum randomness extraction, *Phys. Rev. A* **103**, 062206 (2021).
- [63] X. Liu, Y. Wang, Y. Han, and X. Wu, Quantifying the intrinsic randomness in sequential measurements, *New Journal of Physics* **26**, 013026 (2024).
- [64] M. Padovan, G. Foletto, L. Coccia, M. Avesani, P. Villoresi, and G. Vallone, Secure and robust randomness with sequential quantum measurements, *npj Quantum Information* **10**, 94 (2024).
- [65] A. Tavakoli and A. Cabello, Quantum predictions for an unmeasured system cannot be simulated with a finite-memory classical system, *Phys. Rev. A* **97**, 032131 (2018).
- [66] S. Roy, A. Bera, S. Mal, A. Sen(De), and U. Sen, Recycling the resource: Sequential usage of shared state in quantum teleportation with weak measurements, *Physics Letters A* **392**, 127143 (2021).
- [67] K. Mohan, A. Tavakoli, and N. Brunner, Sequential random access codes and self-testing of quantum measurement instruments, *New Journal of Physics* **21**, 083034 (2019).
- [68] D. Das, A. Ghosal, A. G. Maity, S. Kanjilal, and A. Roy, Ability of unbounded pairs of observers to achieve quantum advantage in random access codes with a single pair of qubits, *Phys. Rev. A* **104**, L060602 (2021).
- [69] H. Anwer, N. Wilson, R. Silva, S. Muhammad, A. Tavakoli, and M. Bourennane, Noise-robust preparation contextuality shared between any number of observers via unsharp measurements, *Quantum* **5**, 551 (2021).
- [70] S. Mukherjee and A. K. Pan, Semi-device-independent certification of multiple unsharpness parameters through sequential measurements, *Phys. Rev. A* **104**, 062214 (2021).
- [71] P. Roy and A. K. Pan, Device-independent self-testing of unsharp measurements, *New Journal of Physics* **25**, 013040 (2023).
- [72] R. Paul, S. Sasmal, and A. K. Pan, Self-testing of multiple unsharpness parameters through sequential violations of a noncontextual inequality, *Phys. Rev. A* **110**, 012444 (2024).
- [73] S. Datta, S. Mal, A. K. Pati, and A. S. Majumdar, Remote state preparation by multiple observers using a single copy of a two-qubit entangled state, *Quantum Information Processing* **23**, 54 (2024).
- [74] M. Curty and N. Lütkenhaus, Intercept-resend attacks in the bennett-brassard 1984 quantum-key-distribution protocol with weak coherent pulses, *Phys. Rev. A* **71**, 062301 (2005).
- [75] H. Bechmann-Pasquinucci, Eavesdropping without quantum memory, *Phys. Rev. A* **73**, 044305 (2006).
- [76] V. Scarani, H. Bechmann-Pasquinucci, N. J. Cerf, M. Dušek, N. Lütkenhaus, and M. Peev, The security of practical quantum key distribution, *Rev. Mod. Phys.* **81**, 1301 (2009).
- [77] R. König, R. Renner, and C. Schaffner, The operational meaning of min- and max-entropy, *IEEE Transactions on Information Theory* **55**, 4337 (2009).
- [78] M. Farkas, M. Balanzó-Juandó, K. Łukanowski, J. Kołodyński, and A. Acín, Bell nonlocality is not sufficient for the security of standard device-independent quantum key distribution protocols, *Phys. Rev. Lett.* **127**, 050503 (2021).
- [79] A. K. Ekert, Quantum cryptography based on bell's theorem, *Phys. Rev. Lett.* **67**, 661 (1991).
- [80] Y. Xiao, Y. X. Rong, S. Wang, X. H. Han, J. S. Xu, and Y. J. Gu, Experimental sharing of bell nonlocality with projective measurements, *New Journal of Physics* **26**, 053019 (2024).
- [81] P. G. Kwiat, K. Mattle, H. Weinfurter, A. Zeilinger, A. V. Sergienko, and Y. Shih, New high-intensity source of polarization-entangled photon pairs, *Physical Review Letters* **75**, 4337 (1995).
- [82] R. Ursin, F. Tiefenbacher, T. Schmitt-Manderbach, H. Weier, T. Scheidl, M. Lindenthal, B. Blauensteiner, T. Jennewein, J. Perdigues, P. Trojek, *et al.*, Entanglement-based quantum communication over 144 km, *Nature physics* **3**, 481 (2007).
- [83] P. Busch, P. Lahti, J.-P. Pellonpää, and K. Ylisen, Measurement, in *Quantum Measurement* (Springer International Publishing, Cham, 2016) pp. 225–260.
- [84] P. Busch, P. J. Lahti, and P. Mittelstaedt, *The quantum theory of measurement* (Springer, 1996).
- [85] T. Lawson, N. Linden, and S. Popescu, Biased nonlocal quantum games (2010), arXiv:1011.6245 [quant-ph].
- [86] I. Csiszar and J. Körner, Broadcast channels with confidential messages, *IEEE Transactions on Information Theory* **24**, 339 (1978).
- [87] M. Christandl, R. König, and R. Renner, Postselection technique for quantum channels with applications to quantum cryptography, *Phys. Rev. Lett.* **102**, 020504 (2009).

[88] A. Leverrier, Security of continuous-variable quantum key distribution via a gaussian de finetti reduction, *Phys. Rev. Lett.* **118**, 200501 (2017).

### Appendix A: Relevant Upper and lower bounds of parameters $\gamma$ , $q$ and $\theta$

To determine the ranges of the parameters  $\gamma$ ,  $q$  and  $\theta$  for which  $r_C > r_{CS}$ , we examine the parameter space that reproduces the observed statistics, particularly the allowable ranges of QBER and CHSH violations between Alice and Bob, as discussed in Sec. II. By constraining the CHSH violations within the interval [2.0965, 2.1213], as prescribed by Eq. (18), we derive the following bounds for  $\gamma$

$$\gamma_{nl} < \gamma < \gamma_{nu} \quad (\text{A1})$$

where

$$\gamma_{nl} = \sqrt{1 - \left[ \frac{\frac{3}{2\sqrt{2}} - \sin \theta + q(\sin \theta - \cos \theta)}{(1-q)\cos \theta} \right]^2} \quad \text{and} \quad \gamma_{nu} = \sqrt{1 - \left[ \frac{1.0482 - \sin \theta + q(\sin \theta - \cos \theta)}{(1-q)\cos \theta} \right]^2} \quad (\text{A2})$$

The bounds  $\gamma_{nl}$  and  $\gamma_{nu}$  must remain within the interval  $[0, 1]$  to ensure the condition  $\gamma \in (0, 1)$  holds. These constraints establish an upper limit for the bias parameter  $q$ . Given  $\gamma_{nl} \in (0, 1)$  and the condition  $q > 1 - q$ , we obtain the following constraint

$$\frac{1}{2} \leq q < q_{u1} \quad (\text{A3})$$

where

$$q_{u1} = \frac{1}{16} \left[ 3(4 - \sqrt{2}) + \frac{4 - 3\sqrt{2}}{x} - (4 + 3\sqrt{2})x + \frac{6\sqrt{2} - (4 + 3\sqrt{2})x}{1 - x - x^2} - \frac{\sqrt{2}(1 - x^2)}{x(1 - x - x^2)} \sqrt{17 - 12\sqrt{2} + 2x^2 + (17 + 12\sqrt{2})x^4} \right] \quad (\text{A4})$$

where  $x = \tan \frac{\theta}{2}$  and  $\theta \in [0.1420, \frac{\pi}{4}]$ . Similarly  $\gamma_{nu} \in (0, 1)$  leads to

$$\frac{1}{2} \leq q < q_{u2}, \quad \text{with } q_{u2} = 1 - \frac{0.0241}{x} - 1.0241x \quad \text{and } \theta \in [0.1085, \frac{\pi}{4}) \quad (\text{A5})$$

Since the upper bound of  $q$  in Eq. (A5) exceeds the upper bound in Eq. (A4) for any  $\theta \in [0.1420, \frac{\pi}{4}]$ , we adopt, without loss of generality, the permissible range of  $q$  specified by Eq. (A4). Next, from Eq. (22), we derive an additional bound on  $\gamma$  based on the QBER

$$0 < \gamma < \gamma_{nu1}, \quad \text{with } \gamma_{nu1} = \frac{0.0026\sqrt{4957 - 5000q}}{1 - q} \quad (\text{A6})$$

To ensure the QBER remains within the permissible limits, we enforce the condition  $\gamma_{nl} \leq \gamma_{nu1} \leq \gamma_{nu}$ . This yields four distinct regions in the parameter space of  $x$  and  $q$ , each corresponding to different combinations of bounds on  $\gamma$ . These regions facilitate the analysis and refinement of the allowed values for  $x$  and  $q$  while maintaining consistency with QBER and CHSH violation constraints.

*Region 1:* When  $\theta \in [0.1541, 0.1926)$  and  $q \in [\frac{1}{2}, q_{u3})$ . Here,

$$q_{u3} = 0.4837 - \frac{0.0917}{x - 0.618} - \frac{0.0163}{x} - 0.5078x + \frac{0.608}{1.618 + x} - \frac{0.5078(1 - x^2)}{x(1 - x - x^2)} \sqrt{(0.0314 + (x - 0.02)x)(0.0328 + (x - 0.0133)x)} \quad (\text{A7})$$

*Region 2:*  $\theta \in [0.1927, 0.7456)$  and  $q \in [q_l, q_{u3})$ . Here,

$$q_l = 0.4806 - \frac{0.0936}{x - 0.618} - 0.5109x + \frac{0.613}{1.618 + x} - \frac{0.0194}{x} - \frac{\sqrt{0.006 - 0.0052x + 0.3062x^2 - 0.1276x^3 + 3.5465x^4 + 0.271x^5 - 8.0357x^6 - 0.1381x^7 + 4.177x^8}}{4x(1 - x - x^2)} \quad (\text{A8})$$

*Region 3:*  $\theta \in [0.7456, 0.7482)$  and  $q \in [q_l, q_{u4})$ . Here,

$$q_{u4} = 0.4848 + \frac{0.0948}{0.6180 - x} - \frac{0.0152}{x} - 0.5152x + \frac{0.6099}{1.6180 + x} - \frac{0.0625}{x(1 - x - x^2)} \sqrt{0.0589 + 3.8822x^2 + 60x^4 - 131.8822x^6 + 67.9411x^8} \quad (\text{A9})$$

*Region 4:*  $\theta \in [0.7482, \frac{\pi}{4})$  and  $q \in [\frac{1}{2}, q_{u4})$ .

Among the four regions identified, Region 2 provides strict upper and lower bounds on both  $q$  and  $\theta$ . We numerically determine the maximum values of  $q_{u3}$  and  $q_l$ . The maximum value of  $q_{u3} = 0.6361$  (denoted as  $q_{um}$ ) occurs at  $\theta_{um} = 0.3544$ , while the maximum value of  $q_l = 0.6018$  (denoted as  $q_{lm}$ ) is achieved at  $\theta_{lm} = 0.3848$ .